Th STZ1 11

Interpretation of Complex Reservoirs - From Outcrops to Superresolution Imaging

T.J. Moser* (Moser Geophysical Services), S. Johansen (Norwegian University of Science and Technology), B. Arntsen (Norwegian University of Science and Technology), E.B. Raknes (Norwegian University of Science and Technology) & S. Sangesland (Norwegian University of Science and Technology)

SUMMARY

Outcrop models are an invaluable help to calibrate seismic imaging techniques and assess their impact on interpretation of exploration and production targets. We investigate reservoir models based on an outcrop at Kvalhovden, east-Spitsbergen, and evaluate images obtained by regular migration and diffraction imaging. Diffraction images demonstrate the potential to enhance image resolution to beyond the traditional Rayleigh criterion and reveal considerable more structural detail. The use of high-frequency and high-resolution data modeling makes these investigations relevant for both production and exploration. The objective of this paper is to increase the awareness of the interpretation community of enhanced resolution capabilities of seismic imaging.

Introduction

Despite significant improvements in seismic technology in recent years (acquisition, processing, imaging), interpretation remains a challenging task. Incorrect interpretation of available seismic data is still the main reason for the low success rate in the exploration business. A rigorous quality control of seismic imaging and its relation to interpretation targets is called for.
Outcrops and outcrop based models provide a useful tool to calibrate seismic images and evaluate their impact on the interpretation of exploration and production targets. Because outcrops have an uncompromising degree of realism and complexity, models derived from them offer most of the important challenges to imaging and interpretation, usually unavailable in synthetic models or models based on subsurface interpretation. Outcrops provide insight into the scale range of subsurface features, in principle at unlimited resolution. In addition, they can be used to rank the importance of various physical and numerical assumptions that underly the seismic imaging, such as: the accuracy and degree of detail of the migration velocity model, the applicability of wave-equation or Kirchhoff migration, the assumption of acoustic versus elastic forward modeling (mode conversions), anisotropy and possible anelastic effects. A popular perception in recent years is that the adequacy of the velocity model is the single most important component in establishing the interpretation value of a seismic image. Outcrop studies are useful to qualify this perception and balance it against views that other components (resolution, illumination, amplitude fidelity) are of similar importance. One of the key questions is to decide *which imaging technique and which set of assumptions gives the best credit to the geological model from the outcrop* (Bertotti et al. 2013; Bertrand et al. 2014; Cronin 2015; Feng et al. 2015).
A case in point is diffraction imaging, which is designed to suppress energy related to main reflectors in an image, and enhance energy related to small-scale structural details important for interpretation. In this paper we present diffraction imaging based on an outcrop model from Kvalhovden (Spitsbergen, Norway; Johansen et al. 1994; Johansen et al. 2007). We compare standard Kirchhoff migration and diffraction imaging against the outcrop data and discuss differences. The advertized added value of diffraction imaging is a much higher resolution; under idealized conditions, it is even possible to achieve superresolution, that is, to recover structural details much smaller than the seismic wavelength (Khaidukov et al. 2004).

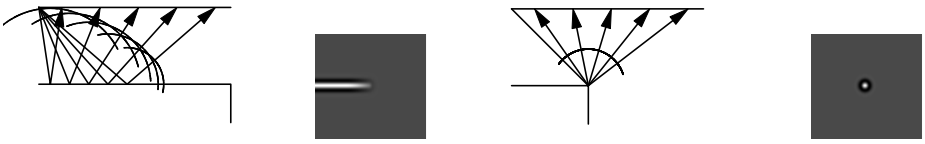

Figure 1 *Reflection and image, diffraction and image (left/right).*

Diffraction imaging

Diffractions are the seismic response from subsurface discontinuities that does not satisfy Snell's specular reflection law. As such, diffractions can be regarded as the carrier of information from small structural elements which are important for interpretation, such as small scale faults, fractures, pinch-outs, salt flanks, reflector unconformities, and in general any small scattering object. The objective of *diffraction imaging* is to isolate this structural information and image it separately from standard migration. In most cases this is done in a pre-stack migration framework, where a migration weight is applied inside the migration loops, suppressing reflection energy that satisfies Snell's law and enhancing diffraction that does not (see Figure 1). Diffraction images are used as a complement to the structural images produced by conventional reflection imaging techniques, by emphasizing small-scale structural elements that are difficult to interpret on a conventional depth image. Two main benefits of diffraction imaging are the capability of high- or even superresolution imaging, and superior illumination (Khaidukov et al. 2004; Moser and Howard 2008; Sturzu et al. 2013). The high-resolution potential of diffraction imaging is demonstrated by several case histories in carbonate reservoirs and unconventional shales, where the diffraction images show much more structural detail than conventional depth migration or coherence (Sturzu et al. 2014). Pelissier et al. (2015) use diffraction imaging to obtain a better fault definition in a field which is highly compartmentalized by complex faulting.

Kvalhovden

The Kvalhovden area is located in eastern Spitsbergen, Norway (Nemec et al., 1987). The geology contains notable synsedimentary collapse features and associated scar-fill deposits have been recognized in an early Cretaceous delta-front succession. The regional stratigraphic and depositional setting was one of a fluvial-dominated delta which prograded south-eastwards across southern Spitsbergen in early Cretaceous time, and subsequently was transgressed by the sea (Figure 2a).
The outcrops at Kvalhovden consist of three main stratigraphic units (Figure 2b). The lower unit is part of a thick sequence of earliest Cretaceous prodelta/delta-slope shaly heterolithic sediments. The second unit is a 100-140 m thick Barremian delta-plain succession, consisting of an extensive sandstone sequence (10-40 m thick) of braided distributary-channel origin at the base, overlain by a sequence of thin, sheet-like to lensoidal sandstones and coal-bearing shales and siltstones, representing interdistributary bay to lagoonal environments. The third and upper unit is an 800 m thick succession of open-marine sandstones and mudshales, whose top at Kvalhovden consists of a distinct barrier-island sandstone unit. The mass transport deposit collapse features in the second unit consist of a series of rotational sandstone slide-blocks (mainly distributary-channel sands) resting on shallowly penetrating faults. The large collapse-scar depressions created by the sliding were initially filled by minor mass-transport of material locally derived from the scar walls, and subsequently by sediments derived mainly from advancing mouth-bar systems which sought to re-establish the delta front.

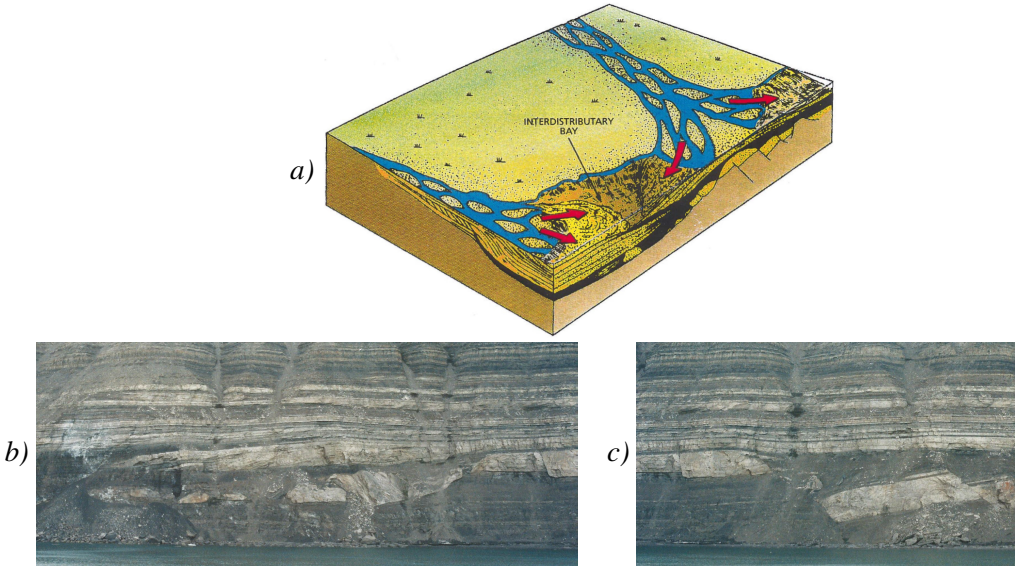

Figure 2 *Kvalhovden. a) Schematic geological model of outcrop area. b/c) Outcrop pictures with collapsed (b) and faulted (c) sandstones.*

Images and interpretation

Velocity and density variations from the outcrops were constrained by photogrammetry and laboratory measurements of rock samples differentiated to lithology (Johansen et al. 2007). Appropriate layer functions were assigned based on well control. This resulted in blocky P-velocity (Figure 3a), S-velocity and density models. An adequately smooth P-velocity model was derived based on a number of test migrations. The depth range is relatively shallow, extending to 500 m. The forward modeling consisted of ray-Born modeling (Moser, 2012) based on a scatter model derived from the difference between the blocky and smooth P-velocity model. The central frequency was 100 Hz and an acquisition was selected with shot spacing 5 m and receiver offsets ranging from 0 m to 1000 m with spacing 10 m. The image grid has horizontal and vertical spacings 0.5 m. We consider this design dense enough to exclude issues with limited coverage. The dominant wavelength in the image area is of the order of 25 m, which gives a yardstick to evaluate the resolution of the images presented here.
Figure 3 shows an overview of the Kvalhovden model, regular Kirchhoff migration and diffraction images. The diffraction images have been obtained by specularity gather construction and tapering at

specularities 99% and 97 % (Sturzu et al. 2013). In this geometry, these can be considered as *weak-* and *strong-taper diffraction images*, respectively, the former being closer to the regular migration and the latter revealing more diffraction detail (and noise).
Figure 4 shows a zoom at the faulted sandstones area and comparison to the outcrop. Here the weak-taper diffraction image (Figure 4b) already contrasts to the regular migration (Figure 4a) because main reflector events are broken up (blue arrow). Compared to the outcrop picture, the strong-taper diffraction image (Figure 4d) seems to better image the outline of the fault blocks (red arrow).
The zoom at the collapsed sandstones area in Figure 5 shows that the strong-taper diffraction image (Figure 5c) reveals details which can be considered as below the traditional resolution criterion of a quarter of the wavelength ($\sim$ 6 m) (see the red and blue arrows in Figure 5). Note that in all images the vertical resolution is higher than the horizontal one. It should also be noted that the modeled seismic data has artificial diffractions because of the gridding of the velocity model, and that not all details in the outcrop have been used in the geomodel.

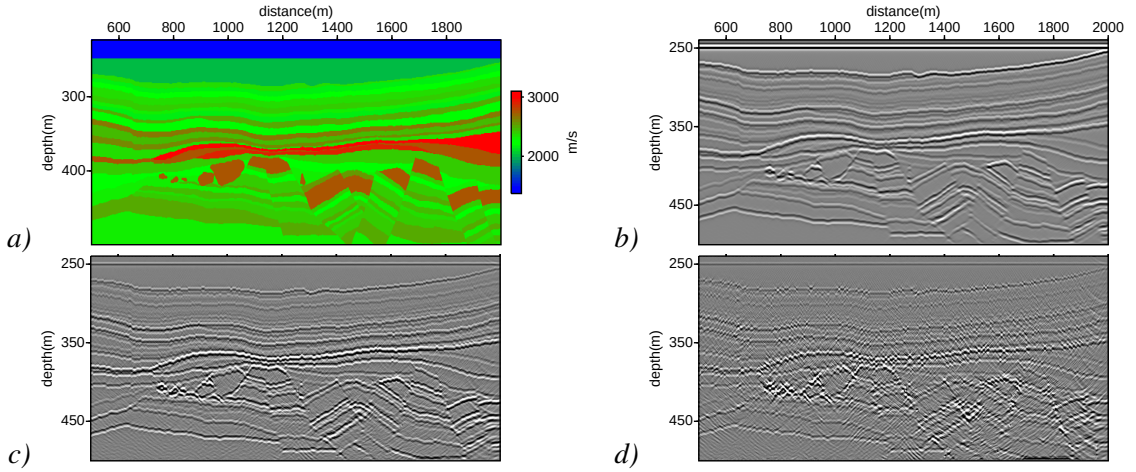

Figure 3 *Kvalhovden. a) P-velocity model, b) regular Kirchhoff migration, c/d) weak/strong taper diffraction image.*

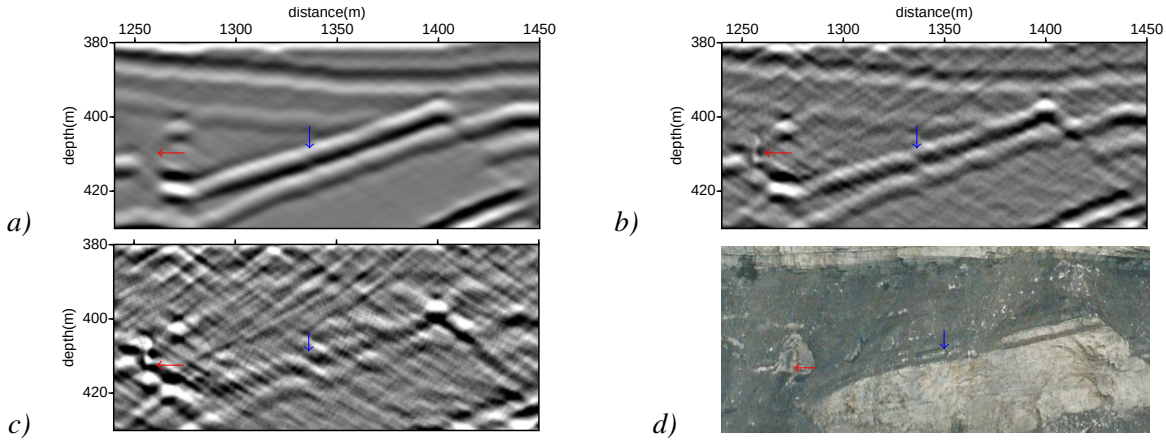

Figure 4 *Zoom on faulted sandstones area. a) regular migration, b/c) weak-/strong-taper diffraction image, d) outcrop picture.*

Conclusions

The outcrop studied here allows to qualify various seismic imaging techniques with respect to their interpretation value on the problem at hand. We compare regular migration with diffraction imaging and demonstrate that the diffraction images reveal more structural detail. Note that by doing this we are willingly committing what is colloquially known as the 'inversion crime', since all detail revealed by the images was already in the velocity model. However, this explicitly serves our objective: *to identify the image technique that gives the best credit to the outcrop*. Due to the high frequencies used in the seismic

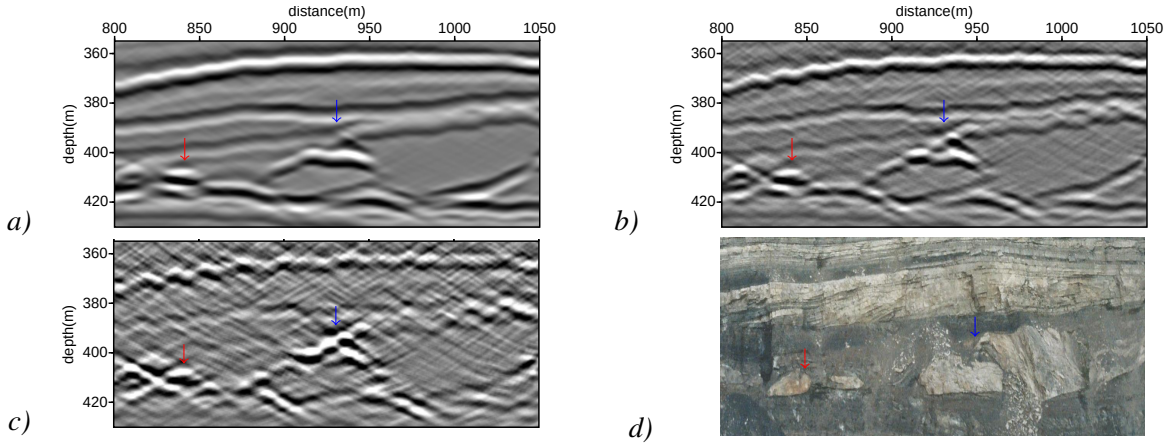

Figure 5 *Zoom on collapsed sandstones area. Same sequence as in Figure 4.*

modelling, the results from the modelled outcrop are probably more relevant for reservoir development cases. However, shallow high-frequent and high-resolution data are now used also for exploration; for example in the Barents Sea. This makes the results from this integrated outcrop study relevant for both production and exploration cases.

References

Bertotti G., Hardebol N.J. and Bisdom K. 2013, Predicting Multiscale Fracture Patterns in Buried Reservoirs: the Importance of Outcrop Data in a Coherent Workflow, *2nd EAGE Workshop on Naturally Fractured Reservoirs*.

Bertrand L., Walter B., Perry G., Geraud Y. and Diraison M. 2014. The Use of Outcrop Analogue Basement Rocks to Help Seismic Imaging of Buried Reservoirs, *76th EAGE Conference Amsterdam*.

Cronin B. 2015. Seismic Expression of Deep-water Slope Channel Complex & Frontal Splay Architectural Elements: Calibration with Outcrop & Sea Floor Analogues from Southern and Eastern Turkey & Various Modern Systems, *Third EAGE Workshop on Rock Physics, Istanbul*.

Feng R., Sharma S., Luthi S.M. and Gisolf A. 2015. An Outcrop-based Detailed Geological Model to Test Automated Interpretation of Seismic Inversion Results, *77th EAGE Conference Madrid*.

Johansen S.E., Kibsgaard S., Andresen A., Henningsen T. and Granli J.R. 1994. Seismic modeling of a strongly emergent thrust front, West Spitsbergen fold belt, Svalbard, *AAPG Bulletin*, **78**, 1018-1027.

Johansen S.E., Granberg E., Mellere D., Arntsen B. and Olsen T. 2007. Decoupling of seismic reflectors and stratigraphic timelines: A modeling study of Tertiary strata from Svalbard, *Geophysics*, **72**, 273-280.

Khaidukov V., Landa E. and Moser T.J. 2004. Diffraction imaging by focusing-defocusing: An outlook on seismic superresolution, *Geophysics*, **69**, 1478-1490.

Moser T.J 2012. Review of ray-Born forward modeling for migration and diffraction analysis, *Studia Geophys. Geod.*, **56**, 411-432.

Moser T.J. and Howard C.B. 2008. Diffraction imaging in depth, *Geophysical Prospecting*, **56**, 627-641.

Nemec W., Steel R.J., Gjelberg J., Collinson J.D., Prestholm E. and Oxnevad I.E. 1988. Anatomy of Collapsed and Re-established Delta Front in Lower Cretaceous of Eastern Spitsbergen: Gravitational Sliding and Sedimentation Processes, *AAPG Bulletin*, **72**, 454-476.

Pelissier M.A., Moser T.J., Jing L., de Groot P., Sirazhiev A., Sturzu I. and Popovici A.M. 2015. Diffraction Imaging of the Zhao Dong Field, Bohai Bay, China, *77th EAGE Conference Amsterdam*.

Sturzu I., Popovici A.M., Tanushev N., Musat I., Pelissier M.A. and Moser T.J. 2013. Specularity Gathers for Diffraction Imaging, *75th EAGE Conference London*.

Sturzu I., Popovici A.M., Pelissier M.A., Wolak J.M. and Moser T.J. 2014. Diffraction imaging of the Eagle Ford shale, *First Break*, **32**, 49-59.